Electronic Supplementary Material (ESI) for Chemical Communications.
This journal is © The Royal Society of Chemistry 2023

Electronic Supplementary Information

A five-stranded heterometallic helicate

Sylvain Sudan,[a] Farzaneh Fadaei-Tirani,[a] and Kay Severin*[a]

[a] *Institut of Chemical Sciences and Engineering, Ecole Polytechnique Fédérale de Lausanne (EPFL), 1015 Lausanne, Switzerland.*

**Email: kay.severin@epfl.ch*

Table of contents

1 General S2
2 Syntheses and characterization S3
3 Mixture of $[Pd(CH_3CN)_4](BF_4)_2$ and L1 (5:2 ratio) S13
4 Addition of L2 to $[Pd_2(L1)_4]^{4+}$ S15
5 Addition of La^{3+} to $[Pd_2(L1)_4]^{4+}$ S18
6 $[Pd_2La(L1)_4]^{7+}$ / $[Pd_2La(L1)_5]^{7+}$ interconversion S21
7 Crystallographic data S23
8 References S26

1 General

All reagents were obtained from commercial sources and used without further purification unless stated otherwise. Ligand **L1** and compound **2** were synthesized following reported literature procedures.[1,2] The syntheses of **1**, **L1** and **L2** were carried out under nitrogen atmosphere.

NMR spectra were measured on a Bruker Avance II spectrometer (^{1}H: 800 MHz) equipped with a 5 mm CPTCI$_{xyz}$ cryoprobe, a Bruker Avance Neo spectrometer (^{1}H: 500 MHz) equipped with a CPTCl$_{xyz}$ 5 mm cryoprobe, a Bruker Avance III spectrometer (^{1}H: 400 MHz) equipped with a BBFO$_z$ 5 mm probe and a Bruker Avance III spectrometer (^{1}H: 400 MHz) equipped with a Prodigy BBO 5 mm cryoprobe. The chemical shifts are reported in parts per million (ppm) using the solvent residual signal as a reference

Routine ESI-MS experiments were carried out on a Xevo G2-S QTOF mass spectrometer (Waters) with a positive ionization mode.

High resolution mass spectrometry experiments were carried out using a hybrid ion trap-Orbitrap Fourier transform mass spectrometer, Orbitrap Elite (Thermo Scientific) equipped with a TriVersa Nanomate (Advion) nano-electrospray ionization source. Mass spectra were acquired with a minimum resolution setting of 120,000 at 400 *m*/*z*. To reduce the degree of analyte gas phase reactions leading to side products unrelated to solution phase, the transfer capillary temperature was lowered to 50 °C. Experimental parameters were controlled via standard and advanced data acquisition software.

2 Syntheses and characterization

2.1 1-Ethynylnaphthalene (1)

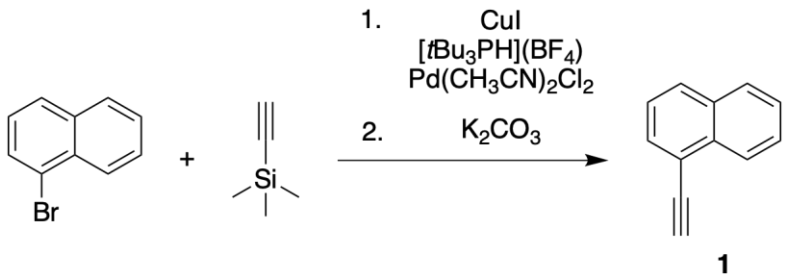

Scheme S1. Synthesis of 1-Ethynylnaphthalene (**1**).

1-Bromonaphthalene (1.43 g, 6.9 mmol, 1.0 eq) was degassed via vacuum/N_2 cycles. Trimethylsilylacetylene (1.25 mL, 9.0 mmol, 1.3 eq.), CuI (57 mg, 0.3 mmol, 0.04 eq.), [*t*Bu_3PH](BF_4) (120 mg, 0.4 mmol, 0.06 eq), Pd(CH_3CN)$_2$$Cl_2$ (65 mg, 0.3 mmol, 0.04 eq.) and 30 mL of a previously degassed dioxane-NEt_3 mixture (3:1) were added under N_2 and the mixture was stirred at 70 °C for 20 h. After cooling-down to room temperature, the mixture was diluted with with EtOAc (30 mL) and filtered through celite. The solvent was evaporated, replaced with DCM (5 mL), and passed through a silica plug. After evaporation under reduced pressure, the residue was redissolved in MeOH (40 mL) and K_2CO_3 (250 mg, excess) was added to the solution. After stirring overnight at room temperature, the suspension was filtered. The solvent was evaporated and the crude product was purified by column chromatography (100% hexane) to give **1** as a red oil (43 % yield). The chemical shifts observed in the ^{1}H NMR spectrum (400 MHz, $CDCl_3$) matched those reported in the literature.[3] **1** was used directly in the next step without any further purification.

2.2 Synthesis of L2

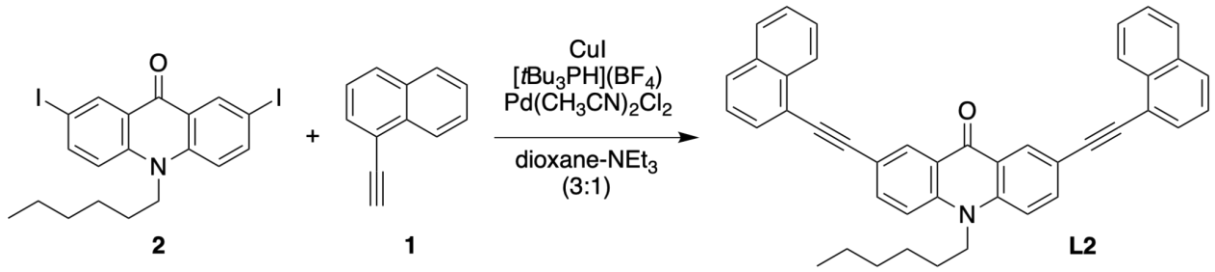

Scheme S2. Synthesis of **L2**.

A mixture of compound **2** (213 mg, 0.40 mmol,1.0 eq.), **1** (183 mg, 1.20 mmol, 3.0 eq.) CuI (8 mg, 0.04 mmol, 0.1 eq), [*t*Bu_3PH](BF_4) (18 mg, 0.06 mmol, 0.15 eq), and $Pd(CH_3CN)_2Cl_2$ (11 mg, 0.04 mmol, 0.1 eq.) were degassed via vacuum/N_2 cycles. 10 mL of a previously degassed dioxane-NEt_3 mixture (3:1) were added under N_2 and the solution was stirred at 80 °C for 24 h. After cooling-down to room temperature, the residue was diluted with $CHCl_3$ (10 mL) and filtered over celite. The solvent was removed under vacuum. The solid was redissolved in DCM (5 mL) and passed through a silica column. The yellow fluorescent fractions (λ_{exc} = 366 nm) were collected and the solvent was evaporated under vacuum. The crude product was recrystallized from hot EtOAc to give **L2** as a yellow solid (68 mg, 29 % yield). ^{1}H NMR (500 MHz, $CDCl_3$, 298 K) δ 8.89 (d, 2H), 8.51 (d,2H), 7.98 (dd, 2H), 7.88 (t, 4H), 7.81 (dd, 2H), 7.65 (ddd, 2H), 7.56 (m, 4H), 7.49 (dd, 2H), 4.41 (t, 2H), 1.99 (m, 2H), 1.65–1.39 (m, 6H), 0.97 (t, 3H). ^{13}C NMR (125 MHz $CDCl_3$) δ 176.91, 141.28, 136.88, 133.40, 133.37, 131.75, 130.58, 128.99, 128.47, 127.08, 126.66, 126.46, 125.46, 122.71, 120.95, 117.03, 115.32, 93.61, 88.25, 46.73, 31.67, 27.43, 26.76, 22.82, 14.18. ESI-MS *m*/*z* calculated for $C_{43}H_{34}NO^+$ $[M+H]^+$ 580.264, found 580.264 .

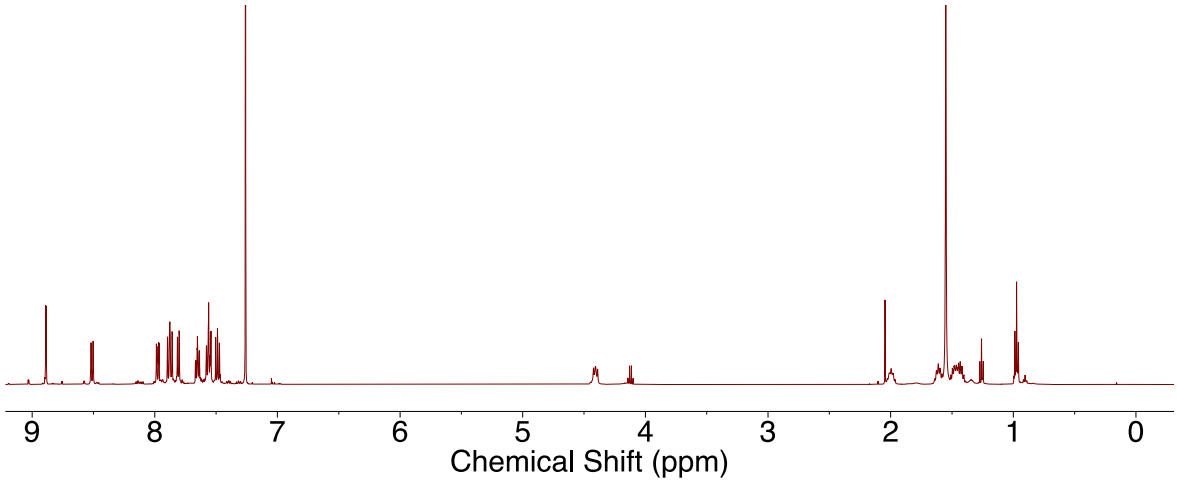

Figure S1. ^{1}H NMR spectrum (500 MHz, $CDCl_3$, 298 K) of **L2**.

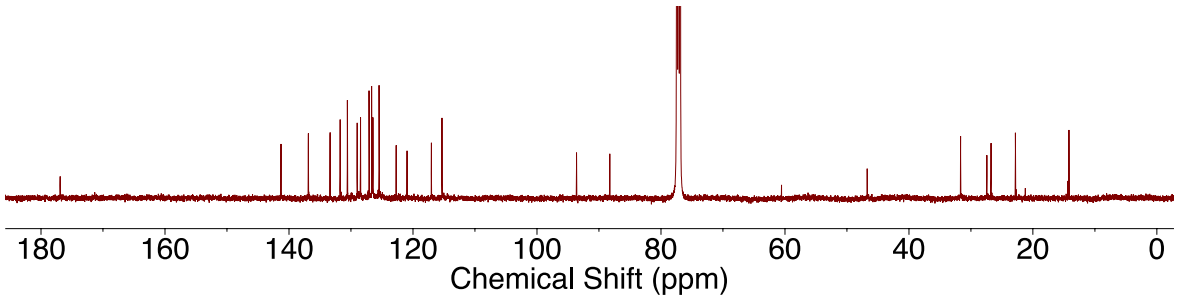

Figure S2. ^{13}C NMR spectrum (125 MHz, $CDCl_3$, 298 K) of **L2**.

2.3 Synthesis of $[Pd_2(L1)_4]^{4+}$

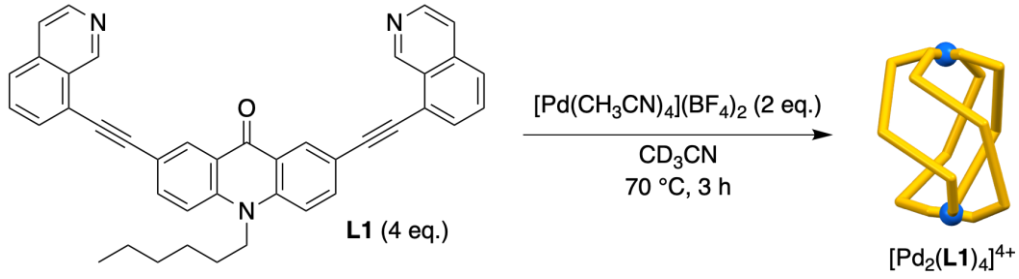

Scheme S3. Synthesis of $[Pd_2(\mathbf{L1})_4]^{4+}$.

The synthesis was adapted from a reported literature procedure.[4] Namely, $[Pd(CH_3CN)_4](BF_4)_2$ (1.5 µmol, 84.6 µL of a 17.8 mM stock solution in CD_3CN, 1.0 eq.) was added to a suspension of **L1** (1.75 mg, 3.0 µmol, 2.0 eq.) in CD_3CN (1 mL) and the mixture was heated at 70 °C for 3 h to give $[Pd_2(\mathbf{L1})_4]^{4+}$ in quantitative yield. The ^{1}H NMR (400 MHz, CD_3CN, 298 K) chemical shifts match with those reported in the literature.[4]

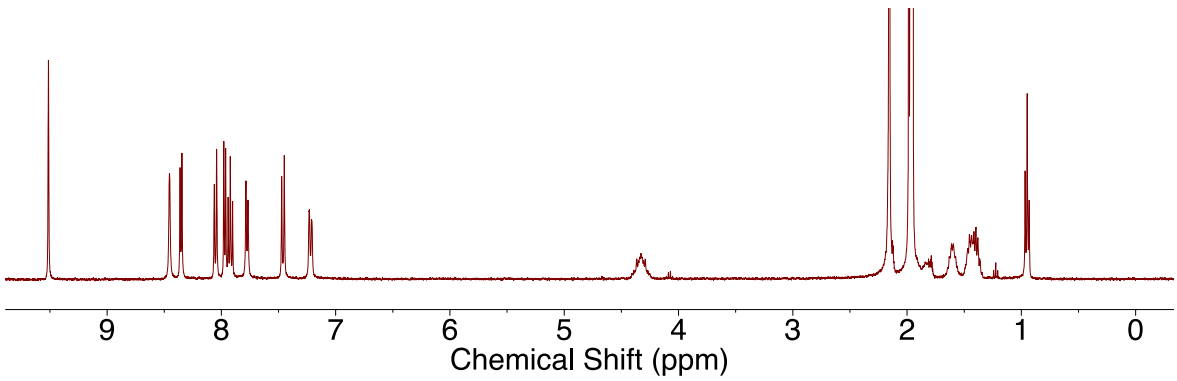

Figure S3. ^{1}H NMR spectrum (400 MHz, CD_3CN, 298 K) of $[Pd_2(\mathbf{L1})_4]^{4+}$.

2.4 Synthesis of $[Pd_2La(L1)_5]^{7+}$

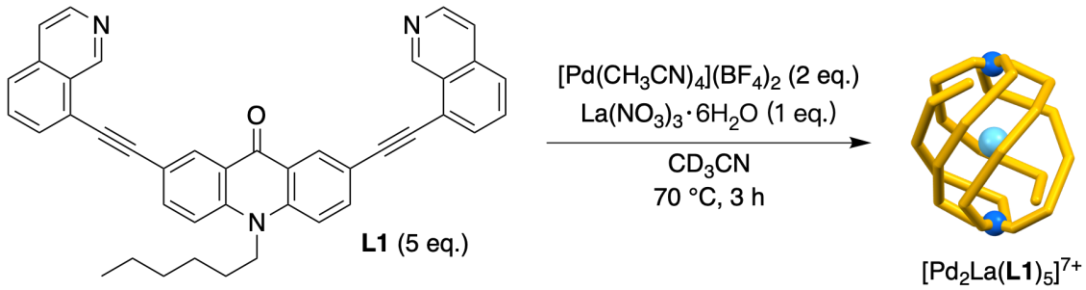

Scheme S4. Synthesis of $[Pd_2La(\mathbf{L1})_5]^{7+}$.

$La(NO_3)_3 \cdot 6H_2O$ (0.7 µmol, 2.02 µL of a 133.9 mM stock solution in CD_3CN, 1.0 eq.) was added to a mixture of $[Pd(CH_3CN)_4](BF_4)_2$ (1.4 µmol, 28.3 µL of a 49.3 mM stock solution in CD_3CN, 2.0 eq.) and **L1** (2.0 mg, 3.5 µmol, 5.0 eq.) in CD_3CN (1 mL). The mixture was heated at 70 °C for 3 h to give $[Pd_2La(\mathbf{L1})_5]^{7+}$. ^{1}H NMR (800 MHz, CD_3CN, 298 K) δ 10.28 (s, 1H), 9.57 (s, 1H), 9.44 (s, 1H), 9.26 (s, 1H), 9.19 (s, 1H), 8.79 (d, 1H), 8.76 (s, 1H), 8.66 (s, 1H), 8.57–8.40 (m, 2H), 8.30 (d, 1H), 8.24 (s, 1H), 8.07 (d, 1H), 8.00 (t, 1H), 7.96 (d, 1H), 7.96–7.93 (m, 2H), 7.90 (d, 1H), 7.86 (t, 1H), 7.82 (d, 1H), 7.74–7.67 (m, 3H), 7.64 (d, 1H), 7.59–7.53 (m, 4H), 7.51 (m, 2H), 7.48–7.41 (m, 2H), 7.26 (t, 1H), 7.23 (d, 1H), 7.12 (d, 1H), 7.00–6.93 (m, 2H),6.91–6.86 (m, 3H), 6.84–6.78 (m, 4H), 6.71 (d, 1H). 4.37–3.91 (m, 6H), 1.73–1.30 (m, 24H), 1.05, (t, 3H), 1.02 (t, 3H), 0.98 (t, 3H). ^{13}C NMR (200 MHz, CD_3CN, 298 K) δ 179.04, 177.70, 177.17, 157.35, 155.66, 154.26, 153.78, 150.51, 145.16, 145.00, 144.81, 144.59, 144.28, 142.49, 142.39, 141.81, 140.76, 140.53, 138.79, 138.09, 137.82, 137.49, 137.18, 137.09, 136.73, 136.41, 136.19, 136.15, 136.05, 135.32, 135.05, 134.88, 134.57, 134.38, 133.12, 132.46, 132.41, 132.34, 132.11, 131.48, 131.20, 130.48, 129.79, 129.63, 129.31, 128.69, 128.27, 128.25, 128.17, 127.99, 127.83, 126.49, 126.12, 126.10, 125.41, 124.89, 122.91, 122.24, 122.06, 121.27, 121.23, 120.95, 120.34, 119.19, 119.63, 119.35, 118.95, 117.82, 117.70, 117.47, 116.37, 116.03, 115.46, 96.43, 95.52, 95.28, 94.92, 93.46, 86.71, 86.49, 85.71, 83.93, 82.73, 48.35, 47.90, 47.59, 32.34, 32.21, 32.06, 28.73, 28.72, 28.25, 26.78, 26.77, 26.62, 23.49, 23.42, 23.33, 14.37, 14.34, 14.30.

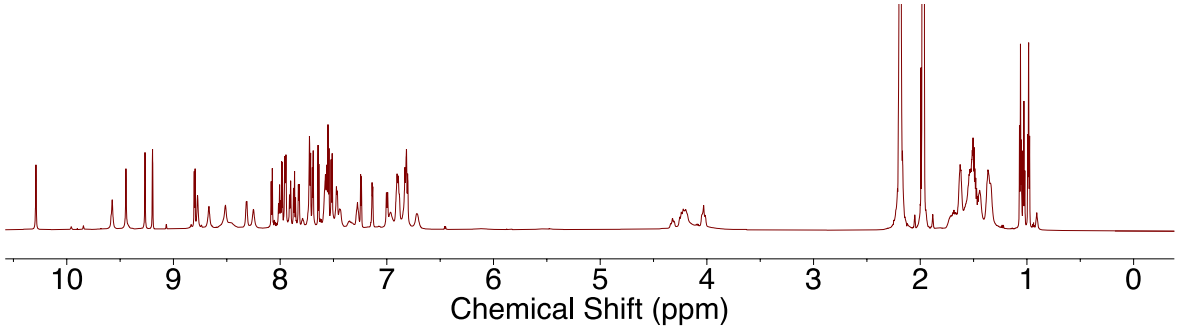

Figure S4. ^{1}H NMR spectrum (800 MHz, CD_3CN, 298 K) of $[Pd_2La(\mathbf{L1})_5]^{7+}$.

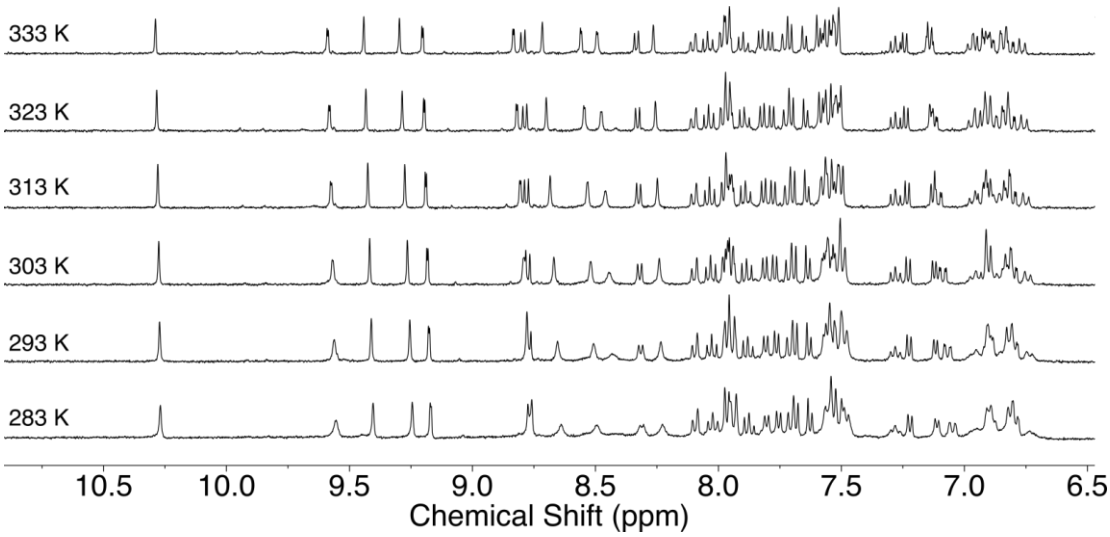

Figure S5. ^{1}H NMR spectrum (400 MHz, CD_3CN) of $[Pd_2La(\mathbf{L1})_5]^{7+}$ recorded at different temperatures.

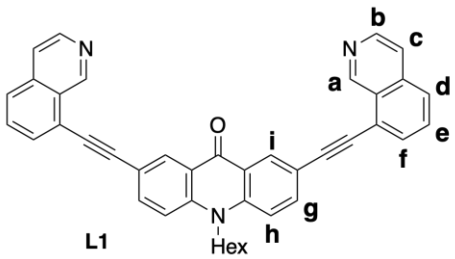

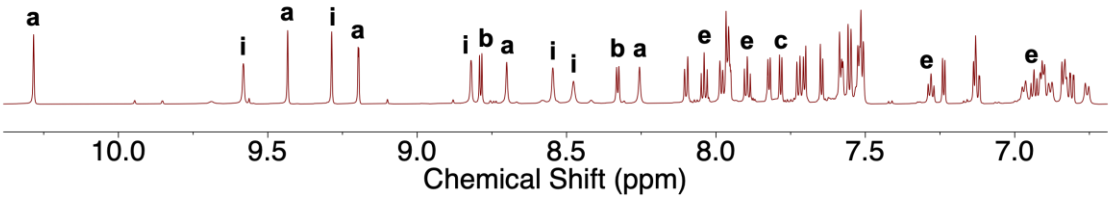

Figure S6. Zoom in the aromatic region of the ^{1}H NMR spectrum (800 MHz, CD_3CN, 323 K) of $[Pd_2La(\mathbf{L1})_5]^{7+}$.

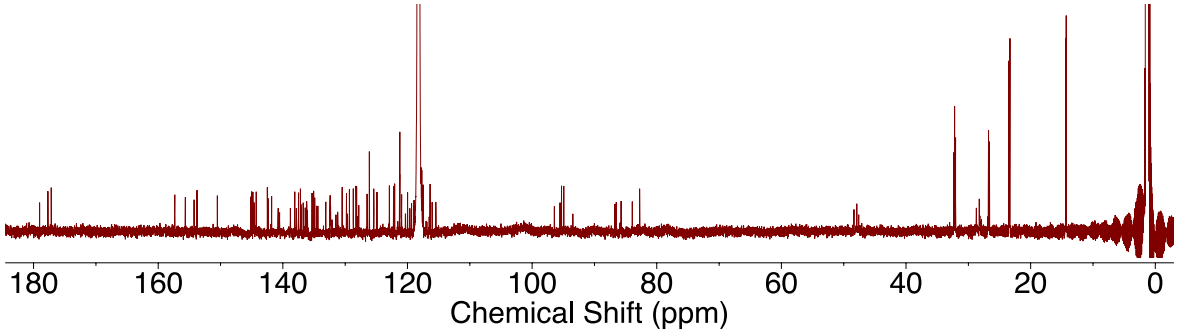

Figure S7. ^{13}C NMR spectrum (200 MHz, CD_3CN, 298 K) of $[Pd_2La(\mathbf{L1})_5]^{7+}$.

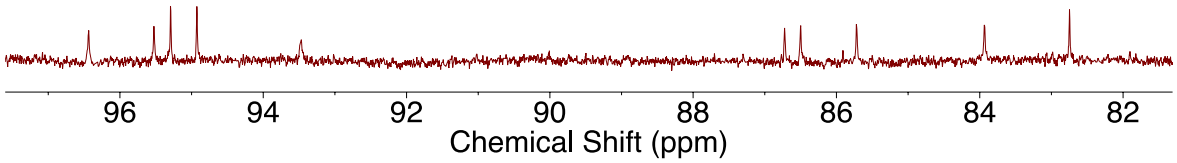

Figure S8. Zoom in the region 81.3 to 97.6 ppm of the ^{13}C NMR spectrum (200 MHz, CD_3CN, 298 K) of $[Pd_2La(\mathbf{L1})_5]^{7+}$. A total of 10 alkyne carbon signals can be observed.

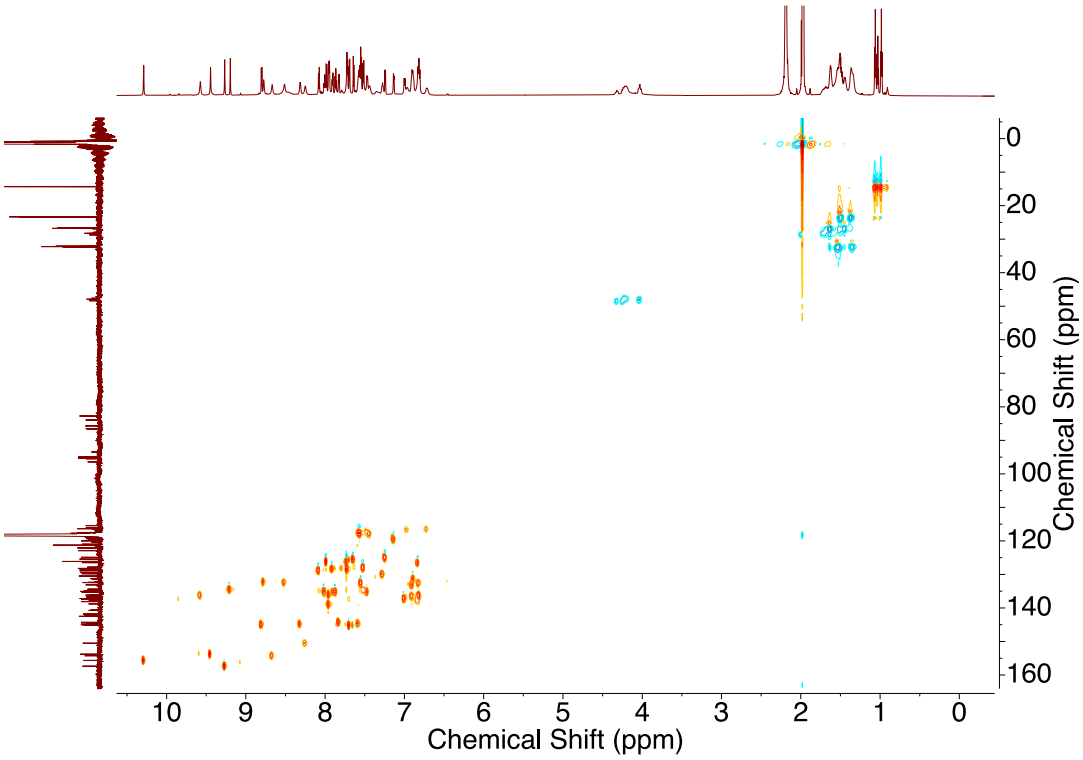

Figure S9. ^{1}H-^{13}C HSQC NMR spectrum (800 MHz, CD_3CN, 298 K) of $[Pd_2La(\mathbf{L1})_5]^{7+}$.

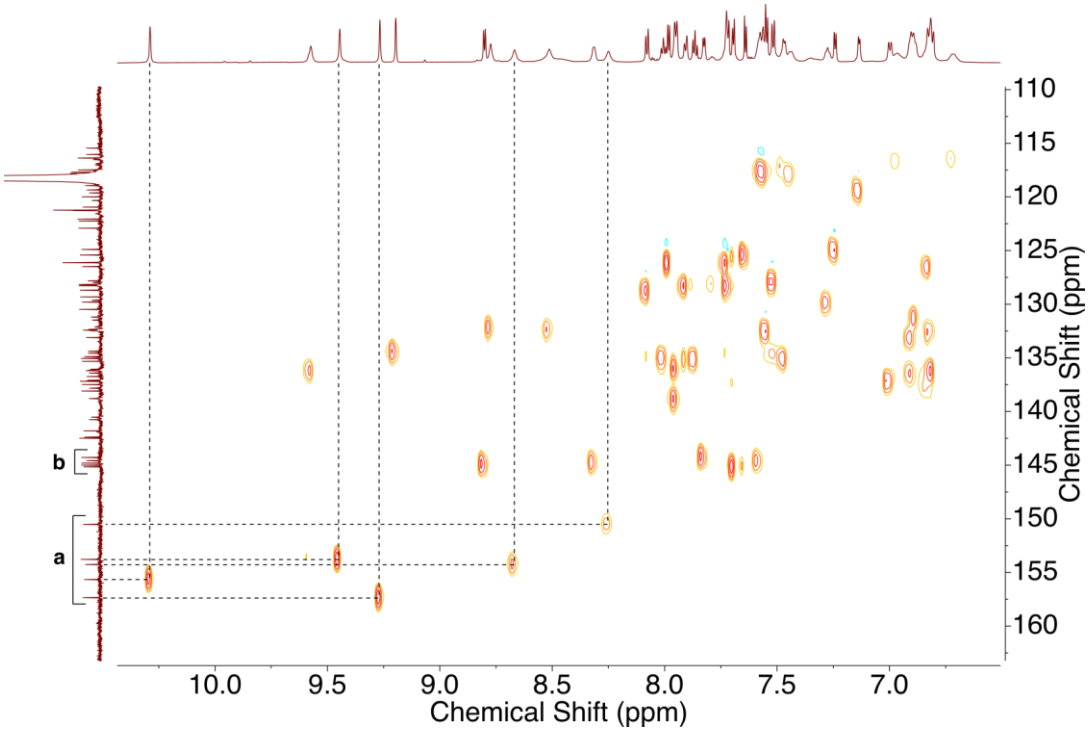

Figure S10. Zoom in the region from 6.5 to 10.4 ppm and 110 to 163 ppm of the ^{1}H-^{13}C HSQC NMR spectrum (800 MHz, CD_3CN, 298 K) of $[Pd_2La(\mathbf{L1})_5]^{7+}$.

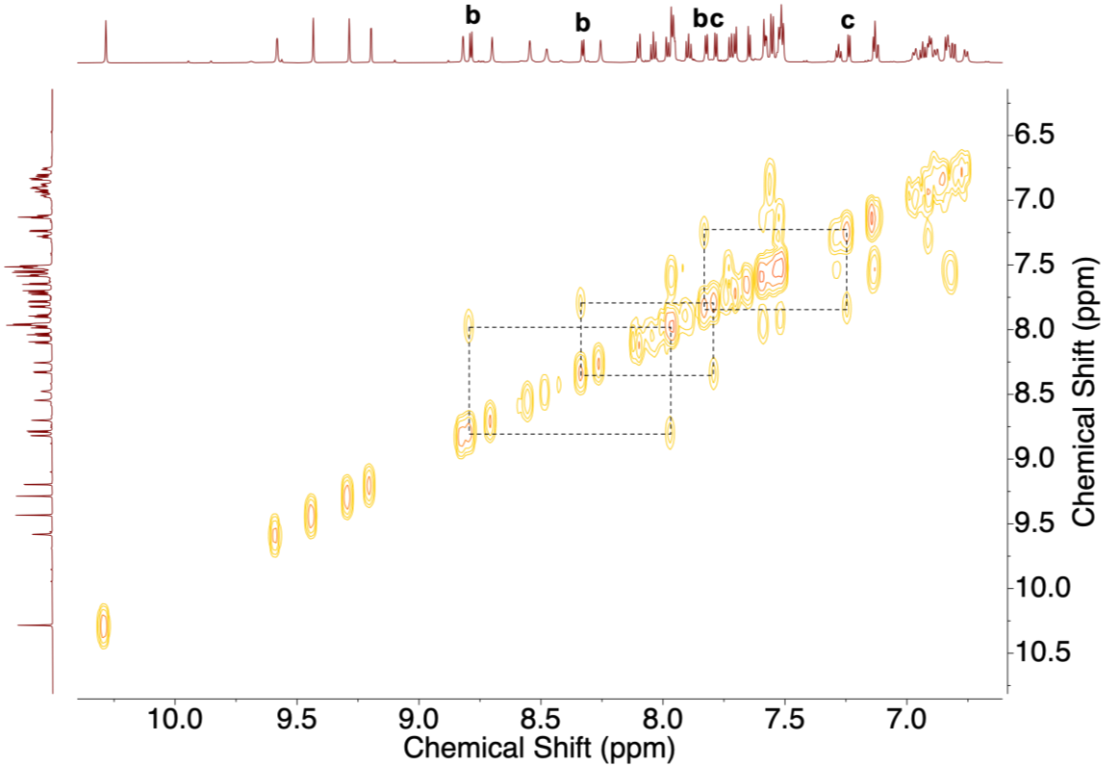

Figure S11. Zoom in the aromatic region of the ^{1}H-^{1}H COSY NMR spectrum (800 MHz, CD_3CN, 323 K) of $[Pd_2La(\mathbf{L1})_5]^{7+}$.

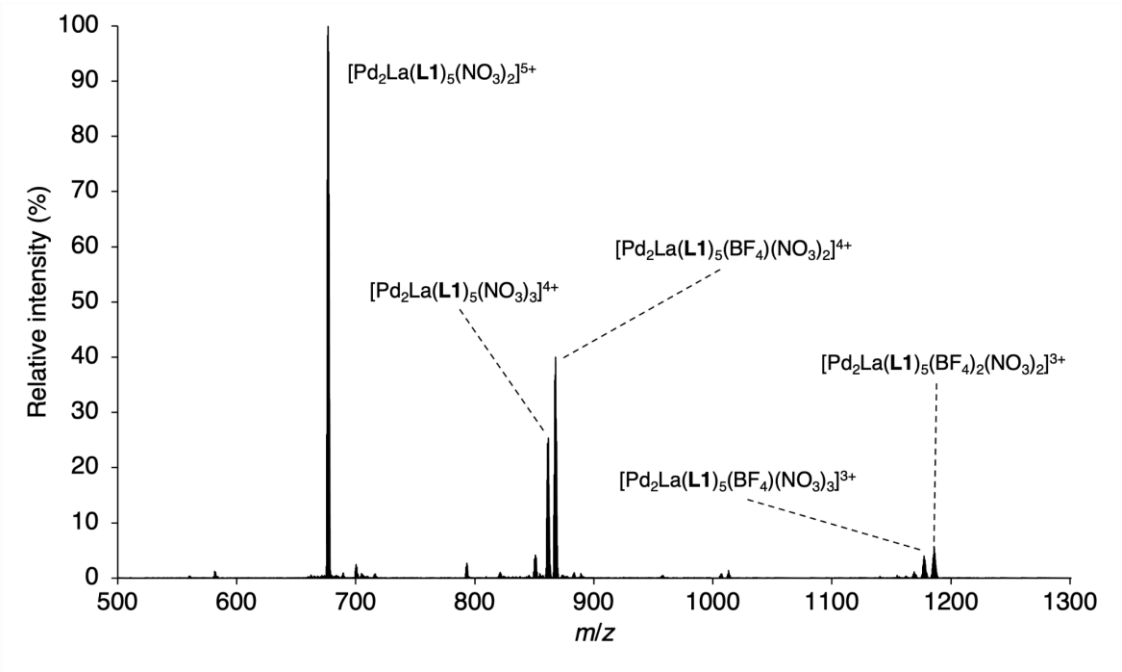

Figure S12. HRMS of a mixture of **L1** (5.0 eq.), $La(NO_3)_3 \cdot 6H_2O$ (1.0 eq.) and $[Pd(CH_3CN)_4](BF_4)_2$ (2.0 eq.) in CD_3CN after equilibration at 70 °C for 3 h.

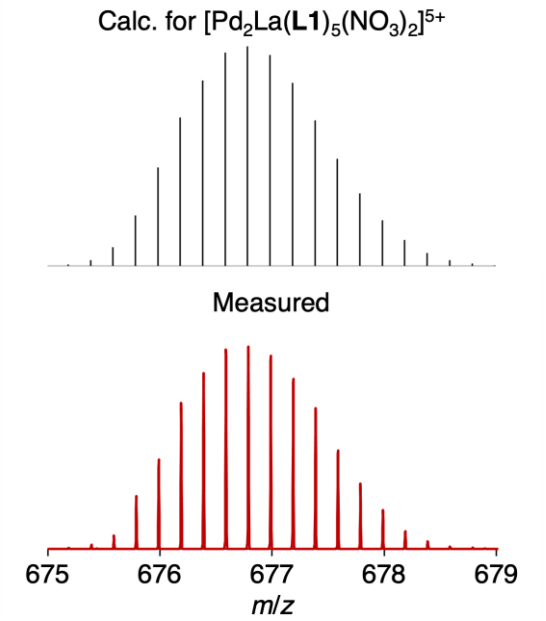

Figure S13. HRMS of a mixture of **L1** (5.0 eq.), $La(NO_3)_3 \cdot 6H_2O$ (1.0 eq.) and $[Pd(CH_3CN)_4](BF_4)_2$ (2.0 eq.) in CD_3CN after equilibration at 70 °C for 3 h, comparing the 675–679 region *m/z* (bottom) and the calculated mass spectrum for $[Pd_2La(\mathbf{L1})_5(NO_3)_2]^{5+}$ (top).

2.5 Isolation of $[Pd_2La(L1)_5(NO_3)_2](BF_4)_4(NO_3)$

$La(NO_3)_3 \cdot 6H_2O$ (2.6 µmol, 26.9 µL of a 97.5 mM stock solution in CD_3CN, 1.0 eq.) was added to a mixture of $[Pd(CH_3CN)_4](BF_4)_2$ (5.2 µmol, 159.6 µL of a 32.8 mM stock solution in CD_3CN, 2.0 eq.) and **L1** (7.6 mg, 13.1 µmol, 5.0 eq.) in CD_3CN (4 mL). The mixture was heated at 70 °C for 12 h and a ^1H NMR spectrum was recorded. The solution was then added to a mixture of pentane/diethyl ether (3:1, 40 mL) and the resulting suspension was centrifuged (4000 rpm, 5 min). The supernatant was discarded and the solid was dried under vacuum to give $[Pd_2La(\mathbf{L1})_5(NO_3)_2](BF_4)_4(NO_3)$ as a yellow/orange solid (8.6 mg, 87 % yield).

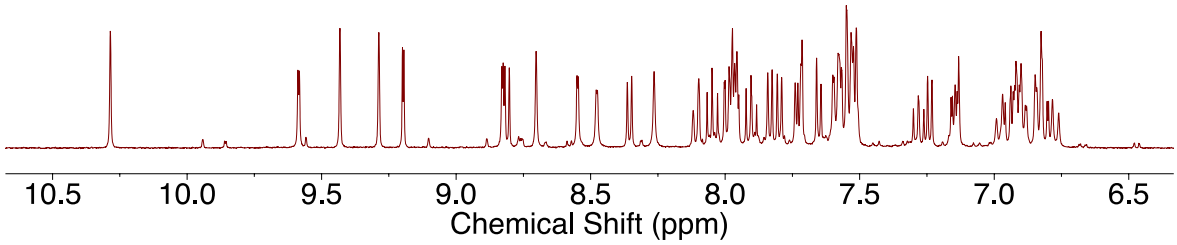

Figure S14. ^1H NMR spectrum (400 MHz, CD_3CN, 323 K) of the isolated $[Pd_2La(\mathbf{L1})_5(NO_3)_2](BF_4)_4(NO_3)$.

3 Mixture of $[Pd(CH_3CN)_4](BF_4)_2$ and L1 (5:2 ratio)

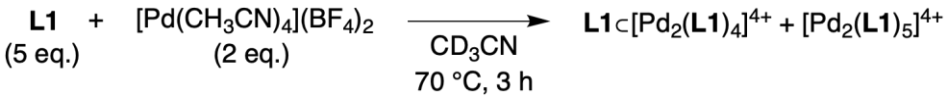

Scheme S5. Equilibration of a mixture of **L1** (5 eq.) and $[Pd(CH_3CN)_4](BF_4)_2$ (2 eq.).

A mixture of **L1** (2.5 mg, 4.4 µmol, 5 eq.) and $[Pd(CH_3CN)_4](BF_4)_2$ (1.8 µmol, 61.1 µL of a 28.6 mM stock solution in CD_3CN, 2.0 eq.) in CD_3CN (1.5 mL) was equilibrated at 70 °C for 2 h.

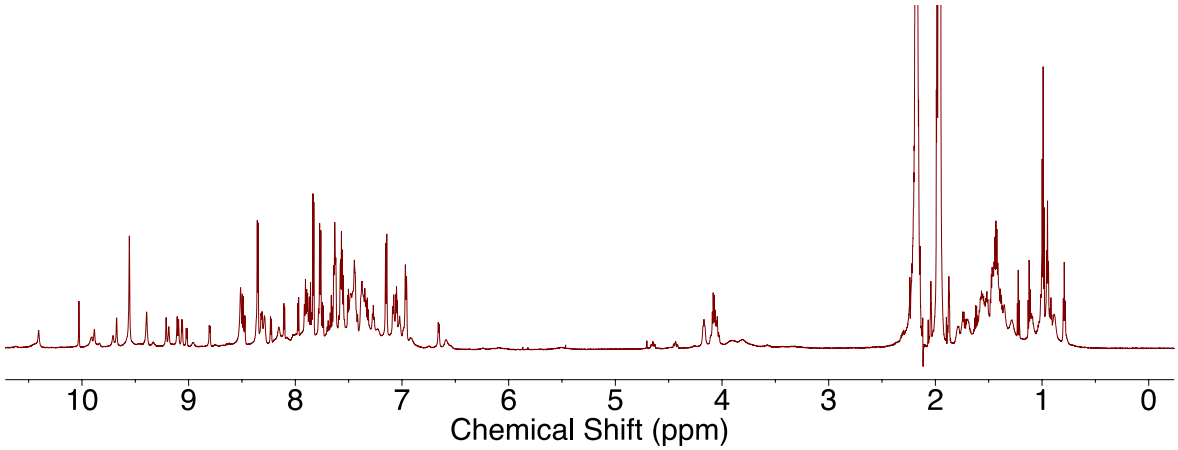

Figure S15. ^{1}H NMR spectrum (800 MHz, CD_3CN) of and equilibrated mixture of **L1** (5 eq.) and $[Pd(CH_3CN)_4](BF_4)_2$ (2 eq.).

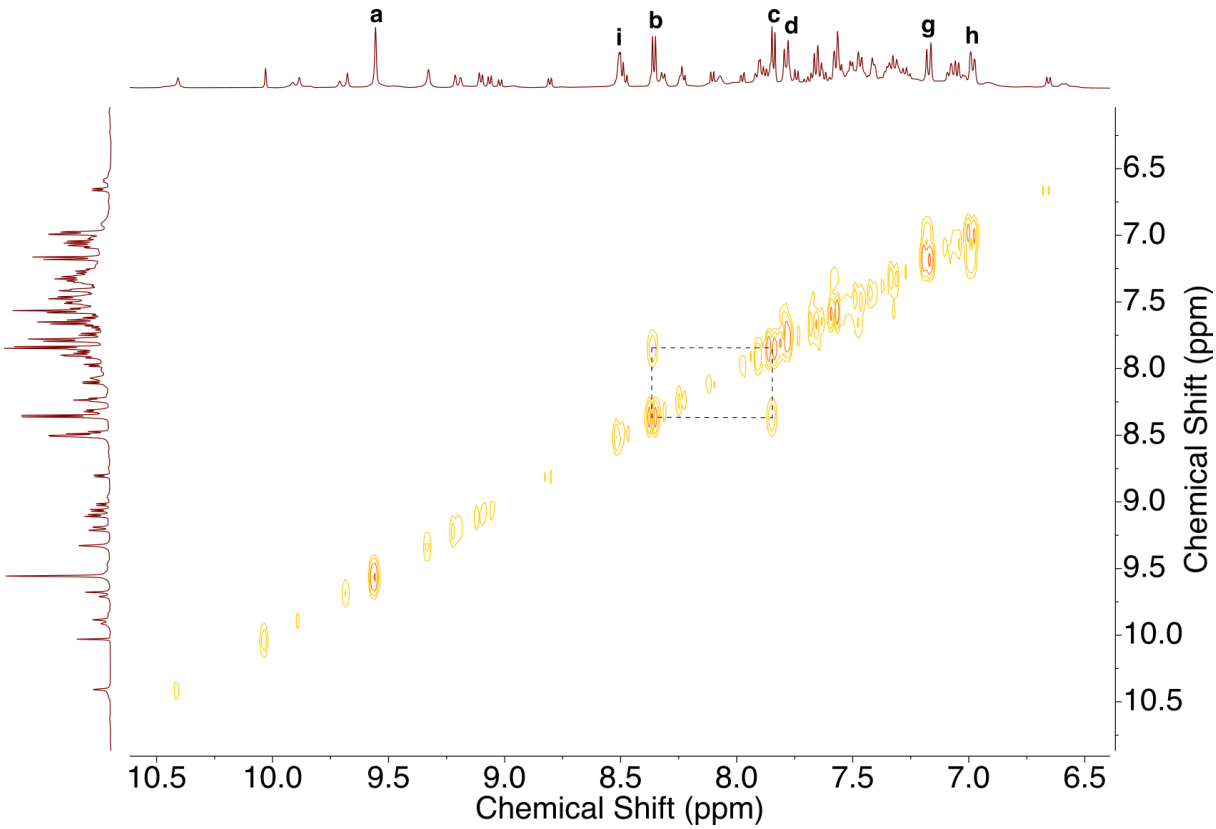

Figure S16. ^{1}H-^{1}H COSY NMR spectrum (500 MHz, CD_3CN) of an equilibrated mixture of **L1** (5 eq.) and $[Pd(CH_3CN)_4](BF_4)_2$ (2 eq.).

4 Addition of L2 to $[Pd_2(L1)_4]^{4+}$

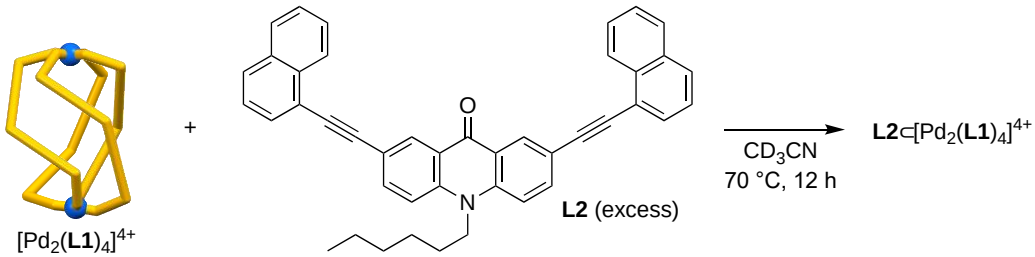

Scheme S6. Equilibration of a mixture of a mixture of $[Pd_2(\mathbf{L1})_4]^{4+}$ and **L2**.

$[Pd_2(\mathbf{L1})_4]^{4+}$ (0.87 µmol, 1078.2 µL of a 0.81 mM stock solution, 1 eq.) was added to a vial containing **L2** (2.0 mg, 3.48 µmol, 4 eq.). The suspension was heated at 70 °C for 12 h while stirring and subsequently filtered.

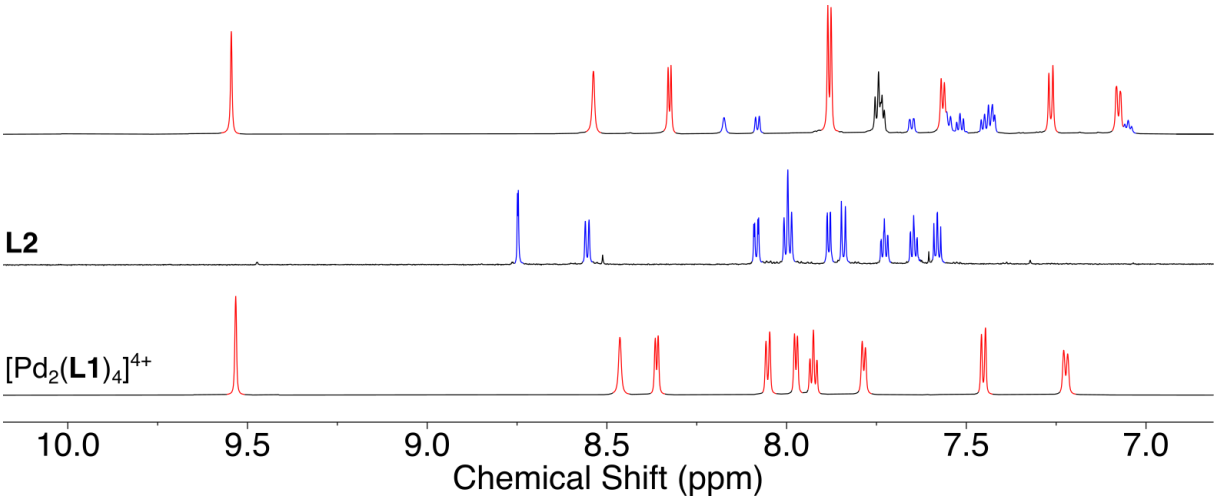

Figure S17. Comparison of the ^{1}H NMR spectra (800 MHz, CD_3CN, 323 K) of an equilibrated mixture of $[Pd_2(\mathbf{L1})_4]^{4+}$ and **L2** (top), **L2** (center) and $[Pd_2(\mathbf{L1})_4]^{4+}$ (bottom).

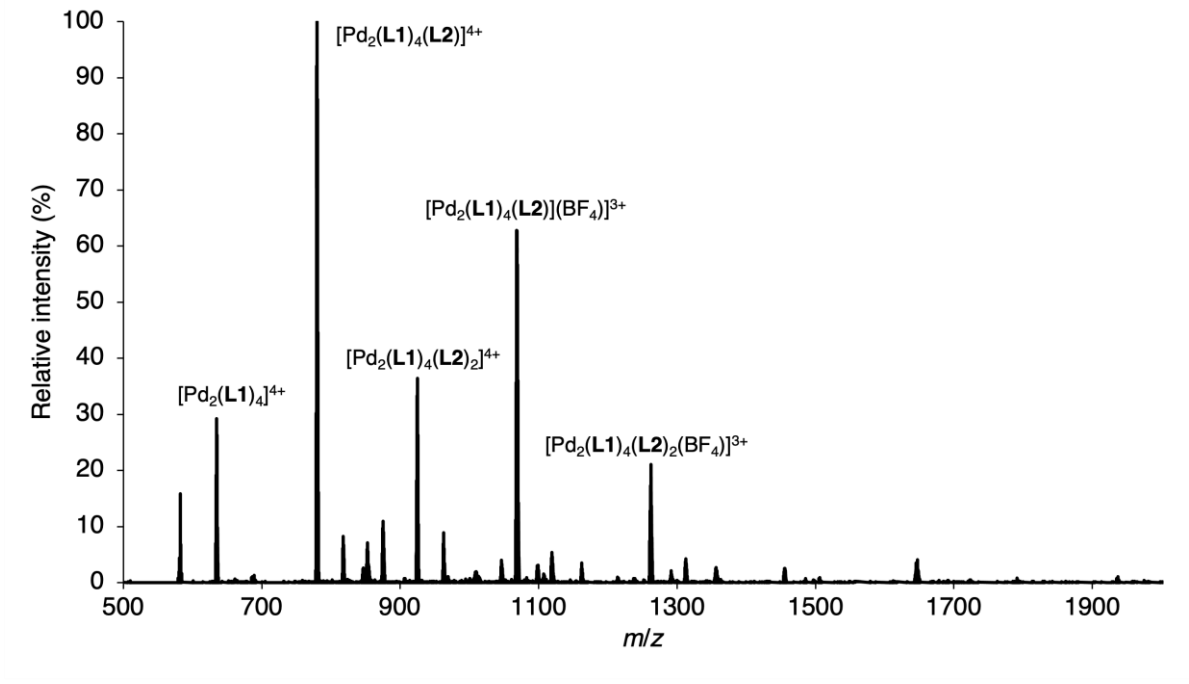

Figure S18. HRMS of an equilibrated mixture of $[Pd_2(\mathbf{L1})_4]^{4+}$ (1 eq.) and **L2** (4 eq.) in CD_3CN.

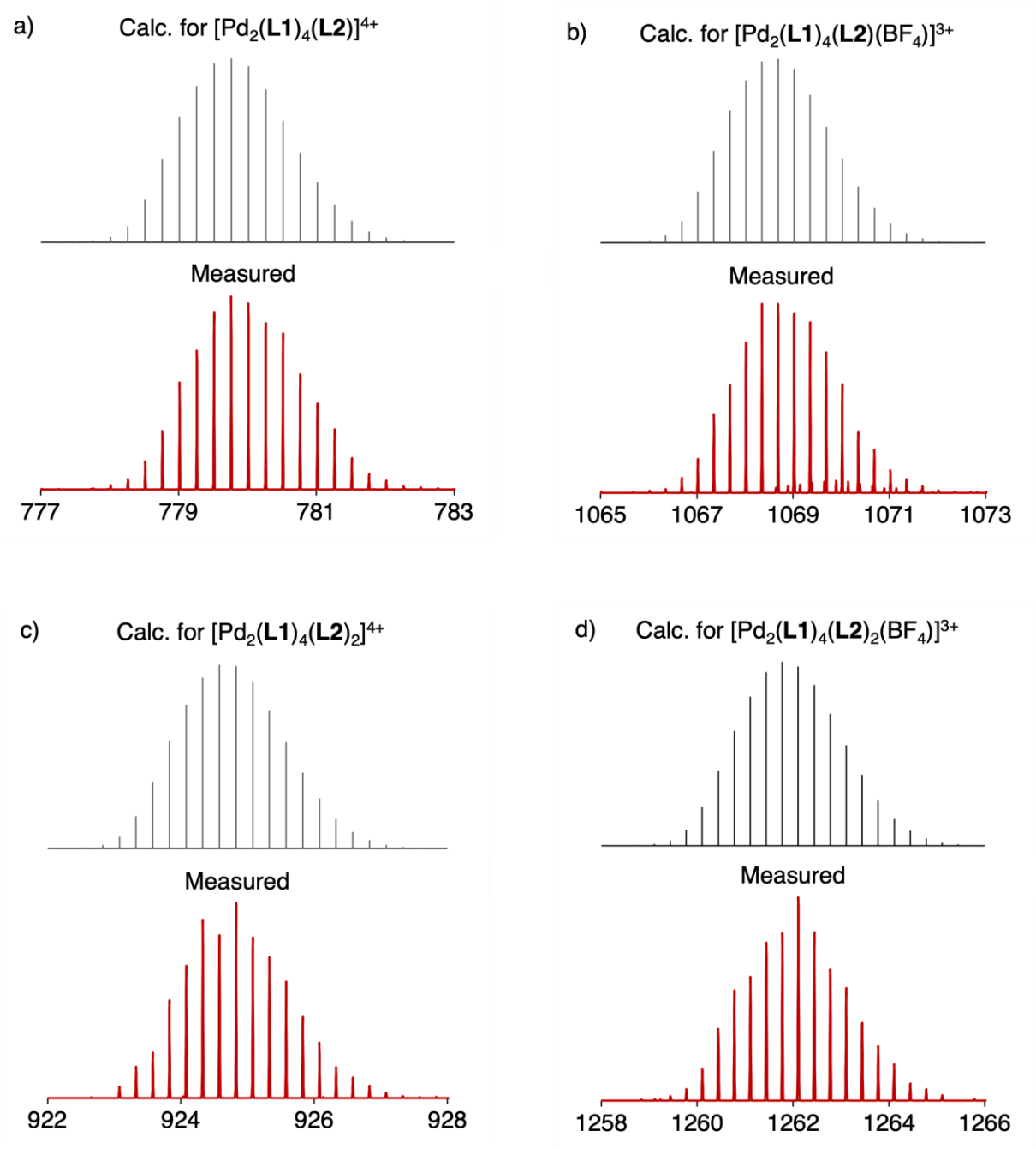

Figure S19. HRMS of a mixture of $[Pd_2(\mathbf{L1})_4]^{4+}$ (1 eq.) and **L2** (4 eq.) in CD_3CN after equilibration at 70 °C for 2 h, comparing the (a) 777–783, (b) 1065–1073, (c) 922– 928, (d) 1258–1266 *m/z* regions (bottom) and the calculated mass spectrum for (a) $[Pd_2(\mathbf{L1})_4(\mathbf{L2})]^{4+}$, (b) $[Pd_2(\mathbf{L1})_4(\mathbf{L2})(BF_4)]^{3+}$, (c) $[Pd_2(\mathbf{L1})_4(\mathbf{L2})_2]^{4+}$ and (d) $[Pd_2(\mathbf{L1})_4(\mathbf{L2})_2(BF_4)]^{3+}$ (top).

5 Addition of La^{3+} to $[Pd_2(L1)_4]^{4+}$

Aliquots (1.6 µL, 0.5 eq.) of a 97.5 mM $La(NO_3)_3 \cdot 6H_2O$ stock solution in CD_3CN were added to an NMR tube containing $[Pd_2(\mathbf{L1})_4]^{4+}$ (400 µL of a 0.8 mM stock solution in CD_3CN, 1.0 eq), to give $[Pd_2La(\mathbf{L1})_4]^{7+}$. ^1H NMR (400 MHz, CD_3CN, 298 K) δ 9.44 (s, 2H), 9.05 (s, 2H), 8.21 (d, 2H), 8.03 (d, 2H), 7.94 (t, 2H), 7.89 (d, 2H), 7.76 (d, 2H), 7.61 (d, 1H), 7.30 (d, 2H), 4.49 (dd, 2H), 1.66 (q, 2H), 1.48 (m, 4H), 0.99 (t, 3H).The ^1H NMR spectra recorded directly after the addition of 0.5 and 1.0 equivalent of La^{3+} are shown below.

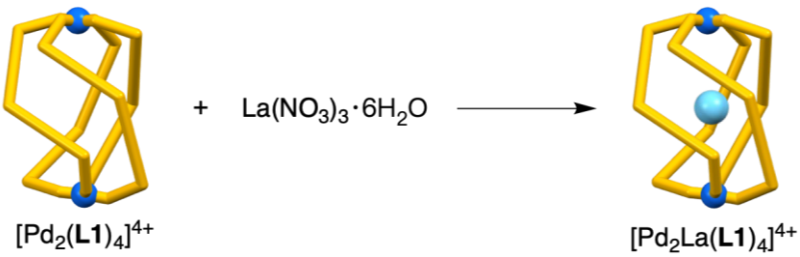

Scheme S7. Addition of La^{3+} to $[Pd_2(\mathbf{L1})_4]^{4+}$.

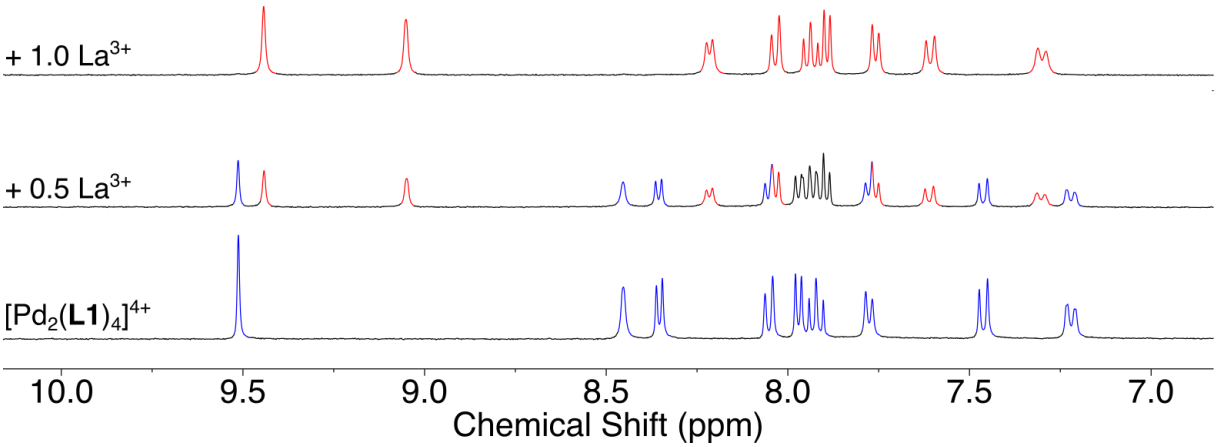

Figure S20. ^1H NMR spectrum (400 MHz, CD_3CN, 298 K) of $[Pd_2(\mathbf{L1})_4]^{4+}$ before (bottom) and after the addition of 0.5 (center) and 1.0 eq. (top) of $La(NO_3)_3 \cdot 6H_2O$. The peaks associated to $[Pd_2(\mathbf{L1})_4]^{4+}$ and $[Pd_2La(\mathbf{L1})_4]^{7+}$ are highlighted in blue and red, respectively.

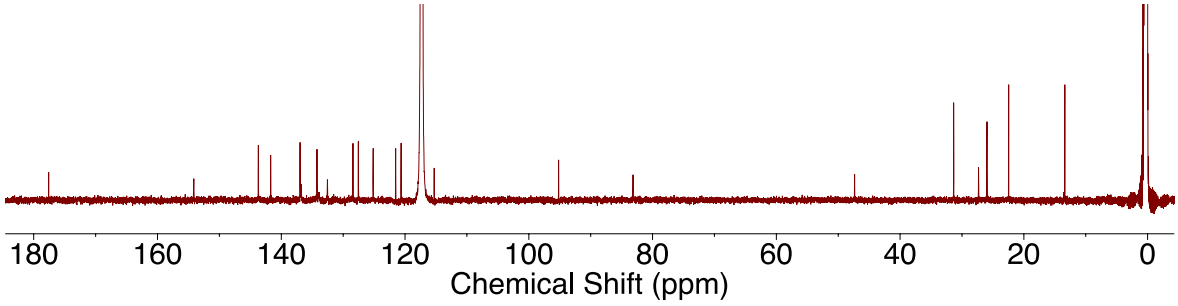

Figure S21. ^{13}C NMR spectrum (200 MHz, CD_3CN, 298 K) of $[Pd_2La(\mathbf{L1})_4]^{7+}$.

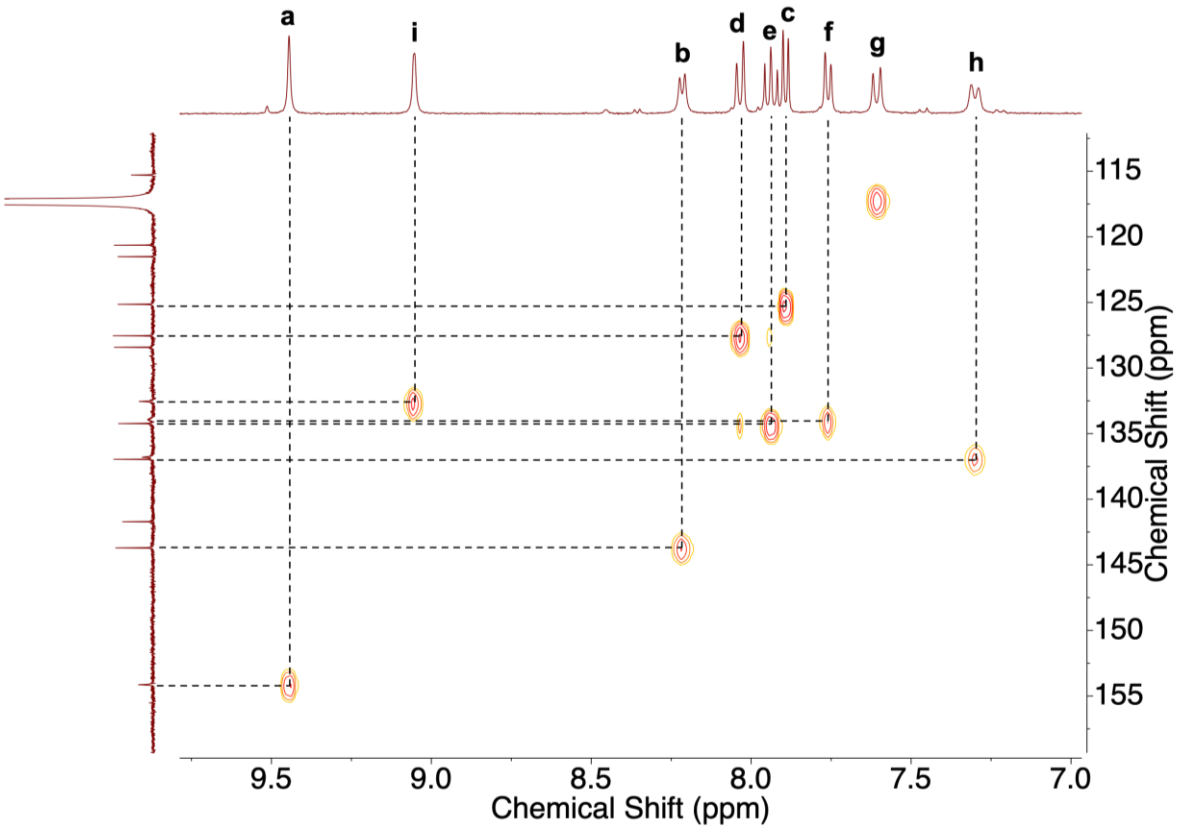

Figure S22. Zoom in the aromatic region of the ^{1}H-^{13}C HSQC NMR spectrum (800 MHz, CD_3CN, 298 K) of $[Pd_2La(\mathbf{L1})_4]^{7+}$.

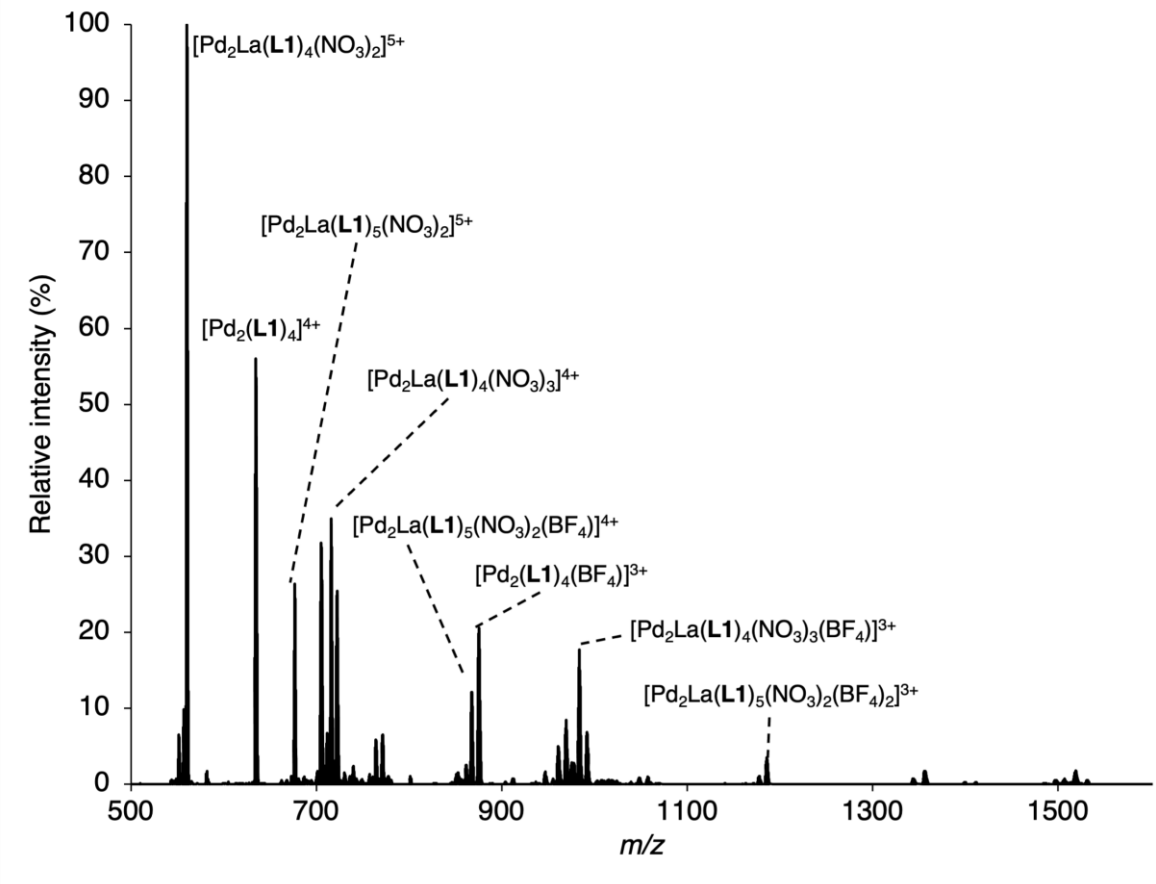

Figure S23. HRMS of a mixture of $[Pd_2(\mathbf{L1})_4]^{4+}$ (1 eq.) and $La(NO_3)_3 \cdot 6H_2O$ (1 eq.) in CD_3CN.

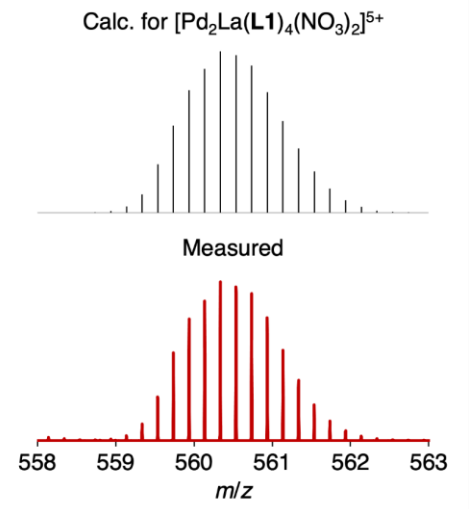

Figure S24. HRMS of a mixture of $[Pd_2(\mathbf{L1})_4]^{4+}$ (1 eq.) and $La(NO_3)_3 \cdot 6H_2O$ (1 eq.) in CD_3CN, comparing the 558–563 *m/z* region (bottom) and the calculated mass spectrum form $[Pd_2La(\mathbf{L1})_4(NO_3)_2]^{5+}$.

6 $[Pd_2La(L1)_4]^{7+}$ / $[Pd_2La(L1)_5]^{7+}$ interconversion

$[Pd_2(L1)_4]^{4+}$ to $[Pd_2La(L1)_4]^{7+}$

$La(NO_3)_3 \cdot 6H_2O$ (1.0 µmol, 10.23 µL of a 97.5 mM stock solution in CD_3CN, 1.0 eq.) was added to $[Pd_2(\mathbf{L1})_4]^{4+}$ (1.0 µmol, 1273.3 µL of a 0.78 mM stock solution in CD_3CN, 1.0 eq.) to give a 0.78 mM stock solution of $[Pd_2La(\mathbf{L1})_4]^{7+}$ (**I**).

$[Pd_2La(L1)_4]^{7+}$ to $[Pd_2La(L1)_5]^{7+}$

$[Pd_2La(\mathbf{L1})_4]^{7+}$ (0.8 µmol, 1022.4 µL of stock solution **I**, 1 eq.) was then added to **L1** (0.46 mg, 0.8 µmol, 1.0 eq.) and the suspension heated at 70 °C for 1 h to give a 0.78 mM solution of $[Pd_2La(\mathbf{L1})_5]^{7+}$ (**II**).

$[Pd_2La(L1)_5]^{7+}$ to $[Pd_2(L1)_4]^{4+}$

Finally, $[Pd(CH_3CN)_4](BF_4)_2$ (0.16 µmol, 5.43 µL of a 28.6 mM stock solution in CD_3CN, 0.5 eq.) and $La(NO_3)_3 \cdot 6H_2O$ (0.08 µmol, 0.80 µL of a 97.5 mM stock solution in CD_3CN, 0.25 eq.) were added to $[Pd_2La(\mathbf{L1})_5]^{7+}$ (0.31 µmol, 400 µL of a 0.78 mM stock solution, 1.0 eq.) and the mixture heated at 70 °C for 1 h to give $[Pd_2La(\mathbf{L1})_4]^{7+}$ (**III**).

^{1}H NMR spectra of the solutions, recorded at each step, are shown below.

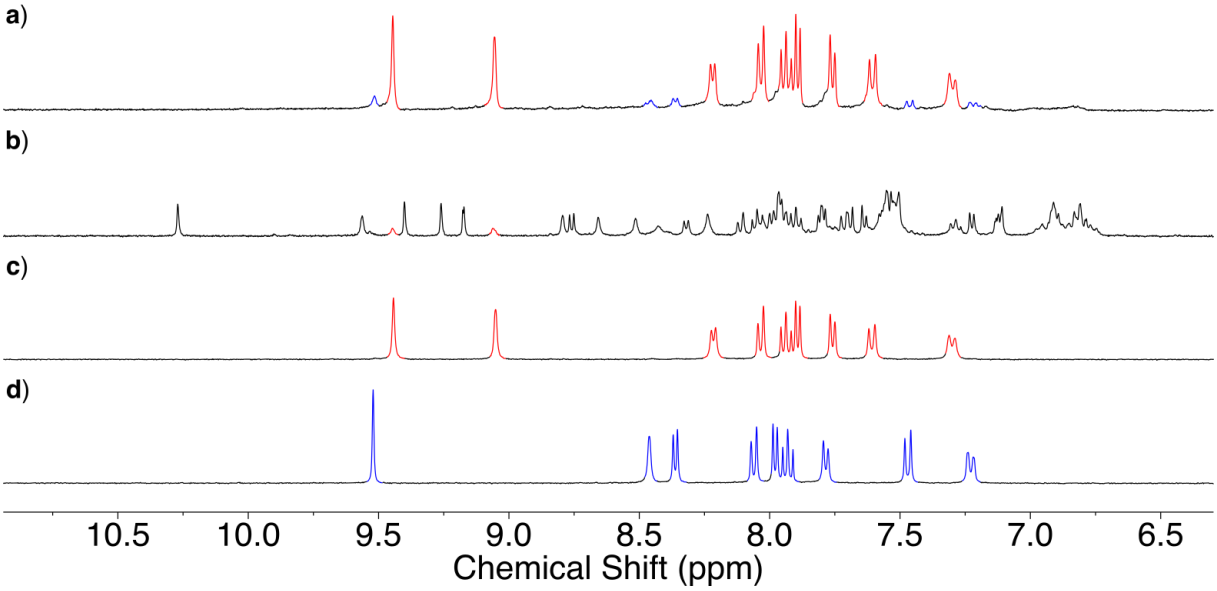

Figure S25. ^{1}H NMR spectrum (400 MHz, CD_3CN, 298 K) of $[Pd_2(\mathbf{L1})_4]^{4+}$ (1 eq.) (**d**) and after the subsequent addition of $La(NO_3)_3 \cdot 6H_2O$ (1 eq.) (**c**), **L1** (1 eq.) (**b**) $[Pd(CH_3CN)_4](BF_4)_2$ (0.5 eq.) and $La(NO_3)_3 \cdot 6H_2O$ (0.25 eq.) (**a**).

7 Crystallographic data

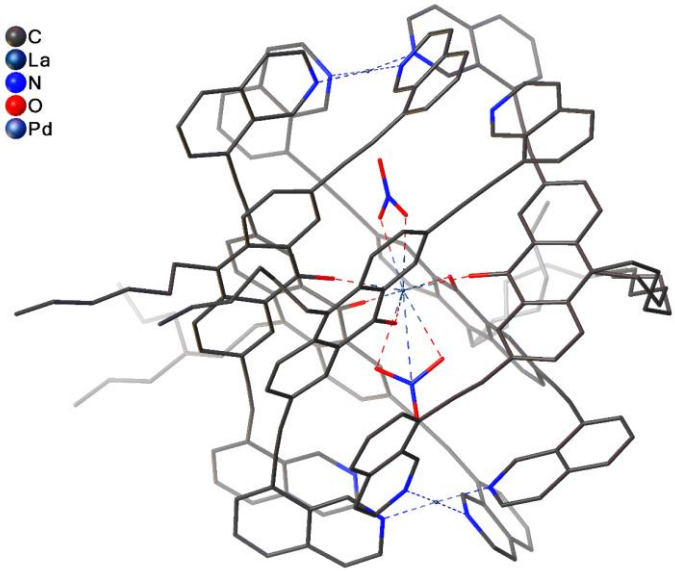

Figure S20. Molecular structure of $[Pd_2La(\mathbf{L1})_5(NO_3)_2]^{5+}$ in the crystal.

Experimental. Single clear intense yellow hexagonal-shaped crystals of $[Pd_2La(\mathbf{L1})_5(NO_3)_2](BF_4)_4(NO_3)$ were used as supplied. A suitable crystal with dimensions 0.11 × 0.06 × 0.06 mm^3 was selected and mounted on an XtaLAB Synergy R, DW system, HyPix-Arc 150 diffractometer. The crystal was kept at a steady T = 140.00(10) K during data collection. The structure was solved with the *ShelXT*[5] solution program using dual methods and by using *Olex2*[6] as the graphical interface. The model was refined with ShelXL[7] using full-matrix least-squares minimisation on F^2.

Crystal Data. $C_{210}H_{155}LaN_{12}O_{11}Pd_2$, M_r = 3374.16, trigonal, $P\bar{3}$ (No. 147), a = 30.9679(6) Å, b = 30.9679(6) Å, c = 34.1539(5) Å, α = 90°, β = 90°, γ = 120°, V = 28365.8(12) $Å^3$, T = 140.00(10) K, Z = 6, Z' = 1, μ(Cu K$_\alpha$) = 3.704, 133335 reflections measured, 33383 unique (R_{int} = 0.0858) which were used in all calculations. The final wR_2 was 0.3158 (all data) and R_1 was 0.0949 ($I \geq 2\sigma(I)$).

Structure Quality Indicators

Reflections:	d min (Cu\a) 2Θ=133.2° 0.84	I/σ(I) CIF 8.9	Rint m=4.00 8.58%	Full 133.2° CIF 99.9
Refinement:	Shift CIF 0.004	Max Peak CIF 1.6	Min Peak CIF -0.8	GooF CIF 0.982

A clear intense yellow hexagonal-shaped crystal with dimensions 0.11 × 0.06 × 0.06 mm^3 was mounted. Data were collected using an XtaLAB Synergy R, DW system, HyPix-Arc 150 diffractometer operating at T = 140.00(10) K.

Data were measured using ω scans with CuKα radiation. The diffraction pattern was indexed and the total number of runs and images was based on the strategy calculation from the program *CrysAlis*^{Pro}.[8] The maximum resolution achieved was Θ = 66.591° (0.84 Å).

The unit cell was refined using *CrysAlis*^{Pro} on 19036 reflections, 14% of the observed reflections.

Data reduction, scaling and absorption corrections were performed using *CrysAlis*^{Pro}. The final completeness is 99.90 % out to 66.591° in Θ. A Gaussian absorption correction was performed using *CrysAlis*^{Pro} numerical absorption correction based on Gaussian integration over a multifaceted crystal model. Empirical absorption correction using spherical harmonics as implemented in SCALE3 ABSPACK scaling algorithm. The absorption coefficient μ of this material is 3.704 mm^{-1} at this wavelength (λ = 1.54184Å) and the minimum and maximum transmissions are 0.754 and 0.904.

The structure was solved in the space group $P\bar{3}$ (# 147) determined by the ShelXT structure solution program using dual methods and refined by full-matrix least-squares minimisation on F^2 using version 2019/3 of ShelXL. All non-hydrogen atoms were refined anisotropically. Hydrogen atom positions were calculated geometrically and refined using the riding model.

There is a single formula unit in the asymmetric unit, which is represented by the reported sum formula. In other words: Z is 6 and Z' is 1.

A solvent mask was calculated, and 1332 electrons were found in a volume of 5697 Å^3*in 8 voids per unit cell. This is consistent with the presence of* 5 $[BF_4]^-$ *per asymmetric unit which account for* 1230 *electrons per unit cell* and the rest are *some solvent molecules of acetonitrile.*

Table 1 Crystallographic data for $[Pd_2La(\mathbf{L1})_5(NO_3)_2](BF_4)_4(NO_3)$

Formula	$C_{210}H_{155}LaN_{12}O_{11}Pd_2$
$D_{calc.}$/ g cm^{-3}	1.185
μ/mm^{-1}	3.704
Formula Weight	3374.16
Colour	clear intense yellow
Shape	hexagonal-shaped
Size/mm^3	0.11×0.06×0.06
T/K	140.00(10)
Crystal System	trigonal
Space Group	$P\bar{3}$
a/Å	30.9679(6)
b/Å	30.9679(6)
c/Å	34.1539(5)
α/°	90
β/°	90
γ/°	120
V/Å^3	28365.8(12)
Z	6
Z'	1
Wavelength/Å	1.54184
Radiation type	Cu$K\alpha$
Θ_{min}/°	2.587
Θ_{max}/°	66.591
Measured Refl's.	133335
Indep't Refl's	33383
Refl's I≥2σ(I)	14532
R_{int}	0.0858
Parameters	2224
Restraints	4049
Largest Peak/e Å^{-3}	1.560
Deepest Hole/e Å^{-3}	-0.832
GooF	0.982
wR_2 (all data)	0.3158
wR_2	0.2537
R_1 (all data)	0.1872
R_1	0.0949
CCDC number	2258906

8 References

1 W. M. Bloch, Y. Abe, J. J. Holstein, C. M. Wandtke, B. Dittrich and G. H. Clever, *J. Am. Chem. Soc.*, 2016, **138**, 13750–13755.

2 M. Krick, J. Holstein, C. Würtele and G. H. Clever, *Chem. Commun.*, 2016, **52**, 10411–10414.

3 D. Sharma, Y. Hussain, M. Sharma and P. Chauhan, *Green Chem.*, 2022, **24**, 4783–4788.

4 W. M. Bloch, J. J. Holstein, W. Hiller and G. H. Clever, *Angew. Chem. Int. Ed Engl.*, 2017, **56**, 8285–8289.

5 G. M. Sheldrick, *Acta Cryst.*, 2015, **A71**, 3–8.

6 O. V. Dolomanov, L. J. Bourhis, R.J. Gildea, J. A. K. Howard and H. Puschmann, *J. Appl. Cryst.*, 2009, **42**, 339–341.

7 G. M. Sheldrick, *Acta Cryst.*, 2015, **C71**, 3–8.

8 CrysAlis^{Pro} Software System, Rigaku Oxford Diffraction, 2022.